A&A 398, 493–499 (2003)
DOI: 10.1051/0004-6361:20021701

Astronomy & Astrophysics

The cold gas properties of Markarian galaxies

R. A. Kandalyan[1,2,3,⋆,⋆⋆]

[1] V. A. Ambartsumian Byurakan Astrophysical Observatory, 378433 Byurakan, Armenia
e-mail: rkandali@bao.sci.am
[2] Isaac Newton Institute of Chile, Armenian Branch, 378433 Byurakan, Armenia
[3] Institute of Astronomy and Space Sciences of the Al Al-Bayt University, PO Box 130040, Mafraq 25113, Jordan

Received 4 June 2002 / Accepted 25 October 2002

Abstract. A sample of 61 Markarian galaxies detected in the CO line was compiled. Using available HI, H_2, optical and radio continuum data, the analysis of the gas kinematics and the star formation properties for this sample of galaxies was performed. The main conclusion can be summarized as follows:
(1) The HI and CO line widths are well correlated. Interaction between galaxies has no influence on the CO line broadening. A rapidly rotating nuclear disk in the galaxy might lead to the CO line broadening with less influence on the HI line.
(2) The atomic and molecular gas surface densities are well correlated with the blue, FIR and radio continuum surface brightness; however, the correlation for molecular component is stronger.
(3) In general, the galaxies with UV-excess (Markarian galaxies) do not differ in their star formation properties from the non-UV galaxies.

Key words. galaxies: ISM – radio lines: galaxies – ultraviolet: galaxies

1. Introduction

On the basis of luminosity alone, it is not possible to conclude whether or not star formation occurs in a burst. The FIR to blue luminosity ratio $L_{\rm fir}/L_{\rm B}$ provides a qualitative measure of the current star formation rate, and it may be strongly affected by extinction, while the gas emission in mm wavelengths is not affected by extinction.

It is well established that in luminous IR galaxies the star formation indicators, such as $L_{\rm fir}/L_{\rm B}$ or the flux density ratio at 60 and 100 microns $f60/f100$ are better correlated with the molecular hydrogen than with the atomic hydrogen content (e.g. Young et al. 1989). The ratio $L_{\rm fir}/M_{\rm H_2}$, where $M_{\rm H_2}$ denotes the molecular hydrogen mass, is usually interpreted as an indicator of efficiency of star formation (SFE) in galaxies. The SFE is independent of the Hubble type (Devereux & Young 1991; Young et al. 1996) but depends on the environment of a galaxy (Sanders et al. 1991; Combes et al. 1994; Young et al. 1996). This dependence is more pronounced in interacting galaxies rather than in isolated ones. For the IR-bright galaxies, there is a linear relation between H_2 and the dust content with SFE depending on the dust temperature of the warm component (Young et al. 1989). However, when longer wavelengths (mm range) were used in determining the dust content in IRAS-Mkn galaxies (Chini et al. 1992a), a strong correlation between $L_{\rm fir}/M_{\rm gas}$ and temperature of the cold dust was found. According to Andreani et al. (1995), the cold dust emission is associated with both the molecular and atomic hydrogen phases.

The CO line area is used to estimate the H_2 gas mass of a galaxy. The line shape and line width of the CO emission involve information on distribution and kinematics of the gas (Krugel et al. 1990; Chini et al. 1992b).

Since molecular gas appears to play a critical role in the star formation process, it is of great importance to perform CO observations for galaxies, in particular for those with active starbursts.

Markarian galaxies exhibit a variety of activities, from starburst to nuclear, and this sample is one of the most suitable samples for investigation of the gas properties and the starburst phenomenon in galaxies. Using available HI, H_2, optical and radio continuum data, we have analyzed the gas kinematics and the star formation properties of 61 Mkn galaxies. How do the gas properties of galaxies with UV- and non-UV-excess compare?

The value of the Hubble constant equal to 75 km s^{-1} Mpc^{-1} is adopted throughout this paper. Section 2 presents a sample of 61 Markarian galaxies detected in the CO(1−0) line. In Sect. 3, the gas-luminosity relations are discussed. The results obtained are discussed in the final section.

⋆ e-mail: kandalyan@yahoo.com
⋆⋆ *Present address*: Institute of Astronomy and Space Sciences of the Al Al-Bayt University, PO Box 130040, Mafraq 25113, Jordan.

Table 1. Sample of 61 Mkn galaxies.

Mkn	i	a_o	V	L_{fir}	L_B	P_R	M_{HI}	M_{H2}	I_{CO}	WHI	WCO	T	Env	Tel	Ref
	(°)	(′)	km s^{-1}	$L_\odot$	$L_\odot$	W Hz^{-1}	$M_\odot$	$M_\odot$	K km s^{-1}	km s^{-1}	km s^{-1}				
2	32	0.73	5476	10.66	10.29		9.45	9.39	7.5	167	106	0	p?	I	1, 2
35	47	1.35	935	9.08	9.21		8.00	7.60	1.0	96	41	3	i	F	3
52	58	2.06	2252	9.80			8.70	8.73	2.3	96	60	−1		F	3
88	0	0.19	9180	10.53	10.32	21.95	9.35	9.81	3.1	121	100	3	i	O	4
91	0	0.89	5101	10.56	10.05		9.40	9.58	6.0	201	113	3	i	O	4
133	28	1.12	2010	9.58	9.81		8.63	8.56	8.2	95	83	4		I	1, 2
158	68	1.73	2070	9.99	10.01	21.04	8.67	9.07	25.3	209	126	1	I		5
171	47	1.89	3033	11.38	10.60	22.83		9.78	60.0		150	9	ia	I	6
188	43	1.75	2404	9.98	10.20	21.41	8.91	9.16	22.8	270	240	5	I		7
201	61	1.61	2511	10.57	10.07	21.74	8.81	9.05	16.4	87	149	10		I	7
213	54	1.63	3115	10.04	10.29	21.36		9.03	10.1		311	1		I	1, 2
231	43	1.22	12300	12.10	10.98	23.70		10.42	16.0		197	5	ia	I	7
266	29	1.16	8358	11.18	10.69	22.82		10.37	4.9		400	7	ia	N	8
273	90	0.81	11274	11.87	10.87	23.30		10.44	19.8		494	4	ia	I	7
281	32	3.15	2227	9.96	10.42	21.07	8.86	9.19	6.8	305	278	3	i	F	9
286	27	0.85	7548	10.86	10.62	21.76	10.17	9.88	5.4	231	175	4	i	O	4
297	40	0.89	4701	10.64	10.38	22.36	9.47	9.26	12.5	366	180	5	ia	NO	10
311	0	0.43	9190	10.70	10.37	21.86	9.12	9.60	1.9	194	124	6	i	O	4
331	51	0.63	5351	11.11	10.07	22.19	9.93	10.06	16.1	264	281	3	ia	O	4
332	24	1.42	2662	10.04	10.30	20.78	8.81	9.25	22.7	80	64	5		I	5
353	60	0.72	4861	10.43	10.25		9.36	9.66	17.6	192	278	5	i	I	1, 2
363	59	3.82	2935	9.76			8.98	8.66	8.2	150		−2		NO	11
404		0.10	1320	9.82		21.25		8.96	11.4		280			F	3
439	12	2.09	988	9.26	9.58	20.24	7.97	9.08	22.5	62	70	1		I	12
496	90	1.37	8785	11.16		22.52	10.01	10.36	4.3	211	100	−3	ia	N	8
518	0	0.48	9506	10.85	10.69	22.36	9.75	10.05	5.0	242	199	10	i	O	4
533	24	1.13	8662	11.08	10.85	23.10	10.00	10.31	4.0	449	145	4	p	N	8
534	60	1.30	5119	10.72	10.60	22.14	9.50	9.75	8.7	286	420	−2	p	O	12
538	44	1.82	2801	10.35	10.26	22.05	9.02	9.03	12.4	163	177	3	ia	I	5
545	52	1.87	4635	10.78	10.79	22.17	9.46	9.60	17.0	376	364	1	p	I	7
575	40	0.81	5295	10.42	10.36	21.48	9.46	9.66	15.0	153	117	1	i	I	1, 2
602	44	1.32	2866	9.94	10.09	21.28	9.04	8.99	10.9	227	194	3.5		I	1, 2
617	30	1.33	4723	11.27	10.44	22.48	9.39	9.56	14.8	250	255	5	ia	I	7
620	44	3.46	1903	9.81	10.26	21.51	8.69	8.95	22.5	354	340	0.5		I	7
691	61	1.50	3297	10.14	10.36	21.62	9.14	9.00	8.4	143	100	4	p	I	1, 2
708	70	2.26	1897	9.74	9.85	21.11	8.65	9.03	27.1	242	197	5		I	5
731	49	2.39	1414	9.26		20.41		8.22	7.5		100	−1	i	I	1, 2
759	40	2.24	2066	9.76	10.16	21.82	8.78	8.70	10.7	208	167	5		I	1, 2
769	64	1.98	1663	9.80	9.98	21.09	8.62	8.31	6.8	207	89	1		I	5
799	62	1.90	3028	10.48	10.39	21.77	9.53	9.70	49.8	314	309	3	ia	I	7
848	60	0.82	12053	11.54		22.83		10.09	7.8		93	−2	ia	I	5
928	42	1.14	7316	11.07		22.65		10.33	5.9		259	−1	ia	N	8
938	74	1.75	5772	11.16		22.51	9.66	9.78	16.7	418	347	3	ia	I	7
1014			48893	12.14		24.01		10.70	0.2		130			N	13
1034	0	0.43	10047	11.33	10.39	22.65	9.94	10.46	26.4	261	450	6		I	7
1040	90	2.87	4914	10.31	10.73		9.59	9.47	1.8	440	500	4		N	14
1050	54	1.10	4853	10.55	10.37	21.60	9.40	9.63	16.7	217	250	1	i	I	1, 2
1066	65	1.79	3605	10.56	10.29	22.02		9.44	19.3		271	−1	p?	I	7
1073	21	1.04	6991	11.05	10.91	22.63	9.49	10.03	8.9	253	260	3	p	O	4
1088	21	1.75	4626	10.61	10.64	22.02	9.37	9.50	13.4	297	377	0	i	I	7
1093	48	1.10	4441	10.71		22.05	9.92	9.74	6.1	359	253	1	p?	S	5
1157	36	1.28	4495	10.09			9.31	9.02	8.0	259	110	0		NO	15
1194	53	1.88	4552	10.64	10.63	21.85	9.36	9.96	40.2	269	291	−2	i	I	7
1259	44	2.00	2159	10.30		21.53		8.46	9.5			−2		NO	11
1341	49	2.21	1132	9.09	9.57	20.14	8.23	7.95	6.4	186	155	6		I	1, 2
1365	40	0.76	5652	10.55	10.16	21.83	9.44	9.59	11.2	180	217	−2	i	I	1, 2
1376	90	2.90	1829	9.86	10.21	22.10	8.63	8.80	17.2	276	286	1		I	5
1379	58	1.46	2585	9.91	10.23	21.48	8.86	8.84	9.4	86	72	1.7		I	1, 2
1405	26	1.37	4963	10.56	10.91		9.48	9.83	11.1	281	280	−3	p?	O	4
1466	43	4.38	1226	9.45	9.96	20.80	8.37	8.47	17.8	201	120	5		I	7
1485	45	3.14	2308	9.73	10.40		8.91	8.79	10.5	286	240	3		I	1, 2

1. Contini (1996); 2. Contini et al. (1997); 3. Young et al. (1995); 4. Kandalyan et al. (1998); 5. Chini et al. (1992b); 6. Solomon et al. (1992); 7. Krugel et al. (1990); 8. Sanders et al. (1991); 9. Jackson et al. (1989); 10. Sofue et al. (1993); 11. Taniguchi et al. (1991); 12. Wiklind & Henkel (1989); 13. Sanders et al. (1988); 14. Heckman et al. (1989); 15. Taniguchi et al. (1990).

2. Results

2.1. A sample of Mkn galaxies detected in the CO line

The flux limited ($f60 < 1.95$ Jy at 60 micron) sample of Mkn-IRAS galaxies contains 155 objects (Kandalyan et al. 1995). In order to investigate the gas properties of Mkn-IRAS galaxies, we have extracted from the literature all the objects detected in the ^{12}CO(1−0) line (until May 2002). The total number of CO detected Mkn galaxies is 65. The galaxies Mkn 463, 551, 673 and 1027 have been detected in the CO line (Gao & Solomon 1999), but the details of the line parameters, such as the CO line intensity and line width, are not presented. For this reason, we did not include these galaxies in our statistics. The optical, FIR and HI data have been extracted from the LEDA and NED[1] databases. Additional HI data are chosen from Martin et al. (1991) and Kandalyan et al. (1997). The environment information on galaxies are taken from Mazzarella & Balzano (1986); Mazzarella et al. (1991); Mazzarella & Boroson (1993); Keel & van Soest (1992). The radio continuum data are chosen from Bicay et al. (1995) except those for Mkn 158, 188, 331, 404, 759, 1466 (Marx et al. 1994) and Mkn 213, 286, 439 (Stine 1992). For the environment and structure of a galaxy the following abbreviations are used: p–pair of galaxies, i–isolated galaxy, ia–interactive galaxy. The notations: I–IRAM 30 m, F–FCRAO 14 m, O–Onsala 20 m, N–NRAO 12 m, NO–NRA 45 m, S–SEST 15 m for the radio telescopes are used. Table 1 presents the list of 61 galaxies and is arranged as follows:

Column 1: Markarian number of galaxy.

Column 2: Inclination angle in degrees (i).

Column 3: Angular diameter a_o in arcmin.

Column 4: Heliocentric radial velocity V, in km s^{-1}.

Column 5: Logarithm of the FIR luminosity $L_{\rm fir}$, in solar units, calculated according to
$\log L_{\rm fir} = 5.5954 + 2\log D + \log(2.58 f60 + f100)$, where $f60$ and $f100$ are the flux densities at 60 and 100 microns respectively, in Jy, and D is the distance to the galaxy in Mpc.

Column 6: Logarithm of the blue luminosity, $L_{\rm B}$, in solar units, calculated according to $\log L_{\rm B} = 12.164 + 2\log D - 0.4 B_{\rm To}$, where $B_{\rm To}$ is the total B magnitude corrected for galactic and internal absorption.

Column 7: Logarithm of the radio continuum power $P_{\rm R}$ at 6 cm, in W Hz^{-1}, calculated according to
$\log P_{\rm R} = 17.078 + 2\log D + \log F_6$, where F_6 is the flux density at 6 cm in mJy.

Column 8: Logarithm of the atomic hydrogen mass, $M_{\rm HI}$, in solar mass, calculated according to
$\log M_{\rm HI} = 5.372 + \log I_{\rm HI} + 2\log D$, where $I_{\rm HI}$ is the integrated HI line intensity in Jy km s^{-1}.

Column 9: Logarithm of the molecular hydrogen mass $M_{\rm H_2}$, in solar mass, which is calculated with use of the formula: $M_{\rm H_2} = 4.78\, L_{\rm CO}$, by taking the conversion factor from the CO emissivity into H_2 column density as $N_{\rm H_2}/I_{\rm CO} = 3 \times 10^{20}$ cm^{-2} (K km s^{-1})$^{-1}$ (Sanders et al. 1991). The CO line luminosity is calculated according to formula: $L_{\rm CO} = 26.6\, D^2({\rm Mpc})\, \theta^2({\rm arcsec})\, I_{\rm CO}$, where θ is HPBW of the radio telescope.

Column 10: Integrated CO line intensity $I_{\rm CO}$ in K km s^{-1}.

Column 11: HI line width WHI, in km s^{-1}, at half of the peak intensity.

Column 12: CO line width WCO, in km s^{-1}, at half of the peak intensity. The line widths are corrected for the galaxy inclination angle.

Column 13: Morphological type (T) as in RC3.

Column 14: Environment and structure of the galaxy.

Column 15: Radio telescope used for the CO line observation.

Column 16: References for CO data. In the following discussion, the correlations were considered as real if the probability of random occurrence is less than 0.05. The flux densities have not been corrected for redshift because all objects, except Mkn 1014, have redshifts much less than 0.1.

2.2. The HI and H_2 gas kinematics

The gas kinematics of Mkn galaxies are studied by means of the statistical analysis of the HI and CO line widths. Figure 1 shows that there is a good correlation between WHI and WCO (correlation coefficient $r = 0.72$ and its significance is $p < 0.0001$). The relation presented in Fig. 1 indicates that the most part of the CO emission is likely to be co-planar with the large-scale galaxy disk. The same result was obtained previously by Heckman et al. (1989) for a sample of Seyfert galaxies. The dispersion in Fig. 1 may be due to several causes. Firstly, the HI observations are usually carried out with a much larger beam width of the radio telescope than that of CO observations. Hence, the number of individual clouds belonging to the beam area is much higher for the HI observations than for CO, so that the HI line width is a mean value from averaging over many clouds and the velocity dispersion among individual clouds may vary from one galaxy to another. Secondly, the dispersion in Fig. 1 could be also due to external and internal causes such as the environment of the galaxy and the starburst activity. It could be partly due to different behaviour of the gas rotation in galaxies. The least square fit of the HI and CO line widths data is

$$WCO = (0.71 \pm 0.10) WHI + (59.4 \pm 41.8).$$

We believe that, due to the gas motion, different samples of galaxies show different slopes in the HI and CO line width relation.

In Table 2 we report mean values of WHI, WCO, their standard deviation and number for different types of galaxies. Sofue et al. (1993) and Tutui & Sofue (1999) have suggested that tidal interaction could disturb the outermost but not the innermost regions of a galaxy. As a consequence, WHI for interacting galaxies will be much broader than that for isolated ones and no difference will be observed in WCO between the two types of galaxies. It can be seen from Table 2 that there are no significant differences between WHI, WCO for isolated and paired+interacting galaxies, although for paired+interacting objects, WHI is slightly higher than for isolated galaxies (458−377 = 81 km s^{-1}). It is noticeable that unclassified galaxies have smaller values of both WHI and WCO than those

[1] The NASA-IPAC Extra-galactic Database (NED) which is operated by the Jet Propulsion Laboratory, Caltech under contract with the National Aeronautics and Space Administration (USA).

Table 2. Mean values of WHI and WCO for Mkn galaxies.

Env	WHI km s^{-1}	SD	N	WCO km s^{-1}	SD	N
Isolated	377	220	9	366	275	10
Paired+ interacting	458	237	15	370	190	22
Unclassified	278	117	20	245	124	20
All	359	200	44	321	195	52

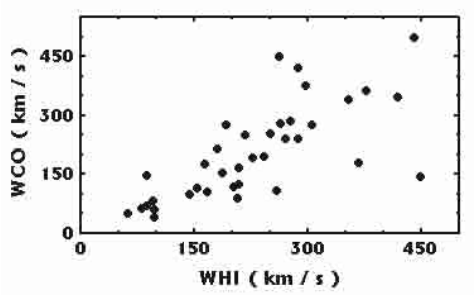

Fig. 1. The HI and CO line widths relation.

of isolated objects and significantly smaller than those for the paired+interacting galaxies. This fact is simply due to observational bias since, on the one hand, these objects are much fainter by global parameters such as $L_{\rm B}$, $L_{\rm fir}$, $M_{\rm HI}$, $M_{\rm H_2}$ (see Table 1) than classified galaxies, and, as a result, they have smaller line widths. On the other hand, because of the relative faintness of these objects, it is difficult to classify them. Nevertheless, when a part of unclassified galaxies were included in the group of isolated objects and another part in the group of paired+interacting galaxies, we still did not find significant differences for WHI and WCO between two main groups. Therefore interaction must have little influence on the HI line broadening and no influence on the CO line broadening in Mkn galaxies, although this problem needs a more detailed investigation based on a statistically significant and homogeneous sample.

The observed integrated CO line profiles in external galaxies result from the convolution of the antenna beam pattern with intrinsic emissivity distribution for which the velocity varies across the beam. The line profile contains information on the distribution and kinematics of the gas.

In general, the HI and CO lines are broadened by the velocity dispersion among individual clouds and/or by galactic rotation. Most of galaxies have an HI line width larger than that of CO. The CO emission is generally concentrated within the central few kpc, while the HI gas distribution shows a depression in the central region of galaxy. The CO gas indicates the rotation and/or velocity dispersion among clouds in the innermost region including any rapidly rotating nuclear disk, whereas the HI gas indicates the rotation and velocity dispersion of the outer disk. Furthermore, superposition of individual clouds in the beam area is higher for HI observations than that for CO. Thus, in general, for a standard rotation curve (e.g. Sofue 1996, 1997, and the comprehensive review of Sofue & Rubin 2001), we should expect an HI line width larger compared to the CO line width. Observationally, there exist galaxies with $FWHM$ of the CO line larger than that of the HI line (Kandalyan 1997; Tutui & Sufue 1999). In these galaxies there may exist a rapidly rotating nuclear disk and/or expanding molecular gas due to the input of kinetic energy from supernovae and stellar winds associated with a starburst (e.g. NGC 1365, 4258). When the molecular gas in the central part of a galaxy has clumpy structure (Sakamoto et al. 1999; Regan et al. 2001), then the velocity dispersion among individual clouds will increase the line width. In the case of lack of the high velocity HI clouds in the central region of a galaxy, the $FWHM$ of the CO line will be larger than that for the HI line. A bar or oval distortion could lead to CO line broadening and increased the star formation activity in a galaxy. Tutui & Sofue (1999) argue that the CO line widths of the fast rotating galaxies tend to be larger than the HI line widths, while the HI line widths of slow rotating galaxies tend to be larger than the CO line widths.

Let us now discuss the difference between the HI and CO line widths. Figure 2 shows the histogram of $(WHI-WCO)$ for Markarian galaxies. One can see that most of galaxies have $WHI > WCO$. However, according to Fig. 2, there exist galaxies with $WHI < WCO$. For the galaxies Mkn 201, 353, 534, 1034, this difference is significant (higher than 0.01) and it is about 0.05 for Mkn 1088 and 1365. The inequality $WCO > WHI$ may indicate the existence of a rapidly rotating nuclear disk in the galaxy and, as a consequence, the rotation curves of these galaxies could have a peak in the central region (<1 kpc), as in case of NGC 3031, 3079, 5236, 6946 (Sofue 1996, 1997). The high angular resolution observations of the HI and CO are essential in testing this hypothesis.

The number of Mkn galaxies with a broad CO line width is insufficient for statistical analysis, but it is interesting that these galaxies are either barred or peculiar objects regardless of whether the galaxy is isolated, interacting or merging. Note that the velocity in barred spirals increases more steeply with radius than in unbarred ones. In the circumnuclear region of barred galaxies, the velocity field of the CO gas can have many different behaviours. For example, the velocity field in NGC 3504 is consistent with purely circular motion (Kenney et al. 1993), while in NGC 4314, both circular and non-circular motions have been observed (Benedict et al. 1996). The disk rotation curves of barred galaxies show dispersion larger than those of normal galaxies (Sofue et al. 1999). Recently Regan et al. (1999) have detected the high velocity (higher than circular velocity) streaming CO gas in seven barred galaxies. Objects with relatively broad CO emission will be very important for the study of the gas kinematics and dynamics of the central region.

3. Gas content – luminosity relation

3.1. Surface densities versus blue surface brightness

In the following discussion we will deal with quantities $S_{\rm HI} = M_{\rm HI}/A$, $S_{\rm H_2} = M_{\rm H_2}/A$, $S_{\rm fir} = L_{\rm fir}/A$, $S_{\rm B} = L_{\rm B}/A$ and $S_{\rm R} = P_{\rm R}/A$ normalized to surface area A of a galaxy instead of $M_{\rm HI}$, $M_{\rm H_2}$, $L_{\rm fir}$, $L_{\rm B}$ and $P_{\rm R}$, in order to avoid the size effect. The blue luminosity is a tracer of the past star formation on the time scale of Gyr, whereas the FIR luminosity is a tracer of

Table 3. Regression coefficients between surface densities and surface brightness. The slope (S), correlation coefficient (r) and probability (p) that there is no correlation between the two variables are indicated in each box. The standard error is indicated in parentheses.

	$\log S_{\rm B}$	$\log S_{\rm fir}$	$\log S_{\rm R}$	$\log S_{\rm HI}$
$\log S_{\rm HI}$	$S = 0.97(0.18)$	$S = 0.45(0.06)$	$S = 0.28(0.08)$	
(all)	$r = 0.64(0.09)$	$r = 0.76(0.08)$	$r = 0.51(0.12)$	
	$p < 3 \times 10^{-6}$	$p < 10^{-6}$	$p < 0.002$	
$\log S_{\rm HI}$	$S = 0.95(0.29)$	$S = 0.65(0.21)$	$S = 0.39(0.26)$	
(isolated)	$r = 0.70(0.19)$	$r = 0.69(0.23)$	$r = 0.50(0.35)$	
	$p < 0.01$	$p < 0.01$	$p = 0.17$	
$\log S_{\rm HI}$	$S = 0.35(0.59)$	$S = 0.57(0.21)$	$S = 0.48(0.26)$	
(paired+	$r = 0.18(0.31)$	$r = 0.65(0.22)$	$r = 0.50(0.27)$	
interacting)	$p = 0.59$	$p < 0.02$	$p = 0.09$	
$\log S_{\rm H2}$	$S = 1.33(0.31)$	$S = 0.73(0.09)$	$S = 0.57(0.10)$	$S = 1.06(0.14)$
(all)	$r = 0.56(0.11)$	$r = 0.78(0.08)$	$r = 0.65(0.10)$	$r = 0.77(0.10)$
	$p < 10^{-4}$	$p < 10^{-6}$	$p < 10^{-6}$	$p < 10^{-6}$
$\log S_{\rm H2}$	$S = 1.23(0.35)$	$S = 0.64(0.22)$	$S = 0.50(0.21)$	$S = 0.87(0.22)$
(isolated)	$r = 0.73(0.19)$	$r = 0.68(0.19)$	$r = 0.64(0.23)$	$r = 0.77(0.18)$
	$p < 0.005$	$p < 0.01$	$p = 0.04$	$p < 0.002$
$\log S_{\rm H_2}$	$S = 0.33(0.53)$	$S = 0.48(0.21)$	$S = 0.36(0.18)$	$S = 0.62(0.17)$
(paired+	$r = 0.20(0.28)$	$r = 0.58(0.24)$	$r = 0.43(0.21)$	$r = 0.75(0.19)$
interacting)	$p = 0.54$	$p < 0.05$	$p = 0.06$	$p < 5 \times 10^{-3}$

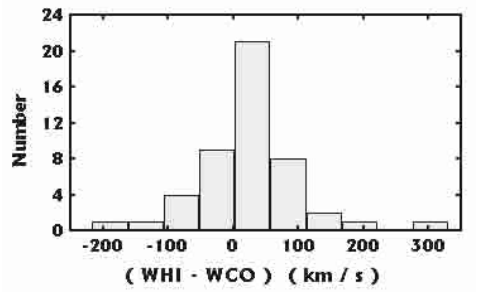

Fig. 2. Distribution of the HI and CO line widths difference.

the recent star formation on the time scale of Myr. We made use of multiple regression analysis to correct the distance effect (Malmquist bias). The corrected regression coefficients are presented in Table 3. In order to have a sufficient number of objects in each morphological group for statistics, we have included paired and interacting galaxies in one group. From Table 3, one can see that the HI and H_2 surface densities are correlated with the blue surface brightness for isolated galaxies only, and correlation between these quantities for the whole sample is completely due to isolated galaxies. We can conclude that, for isolated galaxies, both $S_{\rm HI}$ and $S_{\rm H_2}$ depend linearly on the past star formation activity.

3.2. Surface densities versus surface FIR brightness

Now we discuss the relationships between the gas surface densities and the FIR surface brightness. The corrected regression coefficients are presented in Table 3. The FIR surface brightness is well correlated with the HI and H_2 surface densities for both isolated and paired+interacting galaxies. This suggests that, with an increase in the gas surface density, the FIR surface brightness increases irrespective of the galaxy environment. Another interesting result is the non-linearity of the relation between the HI gas surface density and the FIR surface brightness. This is contrasted with the almost linear relation between the H_2 gas surface density and the FIR surface brightness. This indicates that the recent star formation activity exhibits stronger dependence on the H_2 gas phase than on the HI phase. Furthermore, recently, Wong & Blitz (2002) used the azimuthally-averaged data for seven CO-bright spiral galaxies and found that the SFR surface density exhibits a much stronger correlation with the H_2 gas surface density than with the HI gas surface density. Moreover, there exists a quasi-linear relation between the SFR and H_2 surface densities. Therefore the star-forming gas in these seven galaxies exists predominantly in the molecular form. It should be noted that the mean values of $L_{\rm fir}$, $L_{\rm B}$, $M_{\rm HI}$ and $M_{\rm H_2}$ do not differ significantly for isolated and paired+interacting Mkn galaxies.

3.3. Surface densities versus radio continuum surface brightness

It is well known that the linear relation between the radio continuum and IR emission in galaxies is a consequence of the star formation activity. It is assumed that the cosmic rays arise together with ionizing radiation during the star formation. The ionized gas emits thermal radio emission, while the cosmic ray electrons interacting with a magnetic field emit synchrotron radio emission. Thus, the radio continuum and IR emission are due to the star formation activity. On the other hand, the star formation activity is related to the gas content of a galaxy. Therefore, the study of the relationship between the radio continuum emission and the gas content of galaxies is of interest. The regression coefficients corrected for the distance effect are reported in Table 3. One can see that both phases of the gas are related to the radio continuum surface brightness, but $S_{\rm R}$ is related to $S_{\rm H_2}$ more strongly than to $S_{\rm HI}$. When isolated and paired+interacting galaxies are considered separately, the confidence levels of the relationships are not very high. However,

it could be due to the small number of objects in each group, especially for the group of isolated galaxies (11 objects). Thus, the radio continuum emission in Markarian galaxies is related to both phases of the gas, but the relation to the molecular gas is much stronger than to the atomic one. In general, the results of Sect. 3 are in good agreement with those of Casoli et al. (1996).

4. Discussion

A great number of articles have been devoted to investigation of the gas properties of galaxies (e.g., review by Young & Scoville 1991). In particular, gas-to-luminosity relations of various types of galaxies have been studied extensively. The results of comparison between the gas content and luminosity reveal different effects. For example, in the FIR luminous objects ($\log L_{\rm fir} \gtrsim 10.5$), the HI content is not correlated with the FIR luminosity, while for fainter objects, there exist a strong correlation between these quantities (Kandalyan et al. 1997). In nearby spirals, the HI content is unrelated to the H_2 content (Braine & Combes 1992), whereas in the IRAS-selected galaxies there is a strong correlation between them (see, e.g., present section; Young et al. 1989; Andreani et al. 1995). Thus, gas phase to gas phase and gas phase to luminosity relations in the galaxies are different and very complicated and depend on many internal and external factors such as the environment, luminosity, morphology, star formation history etc.

Up to now, the atomic and molecular hydrogen properties have been investigated on the basis of either optically- or IRAS-selected samples of galaxies. The different samples reveal different gas-to-luminosity relations in the galaxies. For instance, IRAS-selected samples are biased toward galaxies with recent or present star forming activity, while in the optically-selected samples, the past star forming galaxies dominate. In Table 4 we summarized the main results of the comparison of the HI, H_2 surface densities and surface brightness obtained from various samples of galaxies, where B, FIR and R denote the blue, far-infrared and radio continuum surface brightness, respectively. The first line in each box corresponds to $S_{\rm HI}$, and the second line to $S_{\rm H_2}$. The presence of either HI or H_2 indicates the existence of a correlation between the surface density and corresponding surface brightness. "n" indicates the absence of a correlation between two quantities. An empty field means that the relation has not been considered. Bold letters indicate that the considered correlation is stronger than the relationship between the two other variables in the same box. When several articles were available in the literature for each sample, the results were combined and in the references the most recent papers are presented. Table 4 includes only five samples which, in our opinion, represent the main samples studied for the CO emission so far. We have used the following abbreviations: "Nearby" – optically selected nearby galaxies; "Starburst" – optically selected starburst galaxies; "UV-IRAS" – Markarian galaxies detected by IRAS; "IRAS" – IRAS selected galaxies; "Cluster" – clusters' galaxies. These samples are comprised mainly of spiral galaxies. Several important conclusions can be drawn from Table 4. (a) For all samples, the FIR surface brightness is correlated with the molecular hydrogen surface density more strongly than with the neutral hydrogen surface density.

Table 4. Comparison of star formation activities of different samples.

Sample	B	FIR	R	$S_{\rm HI}$	Reference
Nearby	HI	HI	n		1, 2, 3
	H2	**H2**	**H2**	n	
Starburst	HI	HI			4
	H2	**H2**		H2	
UV-IRAS	HI	HI	HI		5
	H2	**H2**	**H2**	H2	
IRAS	HI	HI			6, 7, 8
	H2	**H2**		H2	
Cluster	HI	HI	n		9
	H2	**H2**	**H2**	n	

1. Braine & Combes (1992); 2. Sage (1993); 3. Elfhag et al. (1996); 4. Jackson et al. (1989); 5. Present work; 6. Young et al. (1989); 7. Sanders et al. (1991); 8. Andreani et al. (1995); 9. Casoli et al. (1996).

This suggests that, during present or recent star formation, the molecular phase of the gas plays an immediate part in the star formation.

(b) The strong correlation between the HI surface density and the FIR surface brightness for all samples indicates that, in present or recent star formation, the neutral hydrogen phase is also important. Of course, in some galaxies, a part of the FIR emission could originate in the diffuse atomic medium and not be related to the star formation regions. Thus, we can conclude that both phases of the gas are important for star formation. Casoli et al. (1996) arrived at the same conclusion.

(c) It is clear from Table 4 that both phases of the gas are related to the past star forming indicator $S_{\rm B}$. But now the molecular phase does not dominate in this relation for all samples, as it was in the case of $S_{\rm fir}$. Only in the "UV-IRAS" and "IRAS" samples did $S_{\rm B}$ correlate with $S_{\rm H_2}$ more strongly than with $S_{\rm HI}$. Hence, both components of the gas are important for the past star formation activity.

(d) Unfortunately, the radio continuum data were not available for all samples of Table 4. Nevertheless one can see that there is a strong correlation between $S_{\rm R}$ and $S_{\rm H_2}$. In the "UV-IRAS" sample, the radio continuum surface brightness is correlated also with the atomic hydrogen surface density. The universal correlation between the radio continuum and FIR emission, which is observed from normal galaxies to quasars, is due to the star formation activity (e.g. Kandalyan 1996). Therefore correlation between $S_{\rm R}$ and $S_{\rm H_2}$ has the same origin as the former relation. From this point of view the observed relation between $S_{\rm R}$ and $S_{\rm HI}$ for the "UV-IRAS" sample may indicate that the FIR and HI emissions in these objects are basically due to the star formation while in the "Nearby" and "Cluster" samples a part of the FIR and HI emissions could be related to the diffuse interstellar medium.

(e) It is very difficult to understand the absence of correlation between $S_{\rm HI}$ and $S_{\rm H_2}$ for "Nearby" and "Cluster" samples. In fact, if we believe that both components of the gas are important for star formation, we expect to observe a relationship between them. Perhaps for some samples this relationship is too weak to be observed. But the absence of correlation definitely

does not depend on the environment of a galaxy (field or cluster objects).
(f) Table 4 shows that Markarian galaxies do not differ in star formation properties from other galaxies. The resemblance of "Nearby" and "Cluster" samples is noticeable.

5. Conclusions

The main results of this work may be summarized as follows:
1. A sample of 61 Mkn galaxies detected in the CO(1−0) line was compiled for investigation of the star formation activity. These galaxies were selected from the complete sample of Markarian objects detected by IRAS. The HI, H_2, optical and radio continuum data available from the literature are presented for 61 galaxies.
2. The HI and CO line widths are well correlated. Although the HI line width for interacting objects is slightly larger than that for isolated galaxies, it is proposed that interaction has little influence on the HI line broadening in Markarian galaxies. The galaxy interaction has no influence on the CO line broadening.
3. It was suggested that the rapidly rotating nuclear disk in a galaxy could lead to a CO line width greater than the HI line width.
4. The HI and H_2 gas phases are well correlated with both the past and present star formation indicators such as the blue, FIR and radio continuum surface brightness. However, the molecular phase is related to these indicators more strongly than to the atomic phase. The gas phases are also correlated. In some relations, the isolated and interacting galaxies have different behaviour (see Table 3).
5. In general, the galaxies with UV-excess (Markarian galaxies) do not differ in their star formation properties from the non-UV galaxies.

Acknowledgements. I gratefully thank J.-M. Martin, for his consent to use some unpublished results of observations. It is a great pleasure to thank A. Nikoghossian for the valuable comments. I wish to thank the anonymous referee who helped improve the manuscript. This research has made use of the NASA-IPAC Extragalactic Database (NED) which is operated by the Jet Propulsion Laboratory, Caltech, under contract with the National Aeronautics and Space Administration (USA); the Lyon-Meudon Extragalactic Database (LEDA), supplied by the LEDA team at CRAL-Observatoire de Lyon (France).

References

Andreani, P., Casoli, F., & Gerin, M. 1995, A&A, 300, 43
Benedict, F. G., Smith, B. J., & Kenney, J. D. P. 1996, AJ, 111, 1861
Bicay, M. D., Kojoian, G., Seal, J., Dickinson, D. F., & Malkan, M. A. 1995, ApJS, 98, 369
Braine, J., & Combes, F. 1992, A&A, 264, 433
Casoli, F., Dickey, J., KazŁs, I., Boselli, A., Gavazzi, P., & Baumgardt, K. 1996, A&A, 309, 43
Chini, R., Krugel, E., & Kreysa, E. 1992a, A&A, 266, 177
Chini, R., Krugel, E., & Steppe, H. 1992b, A&A, 255, 87
Combes, F., Prugniel, P., Rampazzo, R., & Sulentic, J. W. 1994, A&A, 281, 725
Contini, T. 1996, Ph.D. Thesis, Universite Paul Sabatier, Toulouse, France
Contini, T., Wozniak, H., Considere, S., & Davoust, E. 1997, A&A, 318, L51
Devereux, N. A., & Young, J. S. 1991, ApJ, 371, 515
Elfhag, T., Booth, R. S., Hoglund, B., Johansson, L. E. B., & Sandqvist, Aa. 1996, A&AS, 115, 439
Gao, Yu, & Solomon, P. M. 1999, ApJ, 512, L99
Heckman, T. M., Blitz, L., Wilson, A. S., & Armus, L. 1989, ApJ, 342, 735
Jackson, J. M., Snell, R. L., Ho, P. T. P., & Barrett, A. H. 1989, ApJ, 337, 680
Kandalyan, R. A. 1996, Afz, 39, 337
Kandalyan, R. A. 1997, Galaxy Interaction at Low and High Redshift, IAU Symp. 186, ed. J. Barnes, & D. B. Sanders (Kluwer Academic Publishers), 84
Kandalyan, R. A., Martin, J.-M., Bottinelli, L., & Gouguenheim, L. 1995, Afz, 38, 639
Kandalyan, R. A., Martin, J.-M., Bottinelli, L., & Gouguenheim, L. 1997, unpublished
Kandalyan, R. A., Martin, J.-M., Horellou, C., Bottinelli, L., & Gouguenheim, L. 1998, unpublished
Keel, W. C., & van Soest, E. T. M. 1992, A&AS, 94, 553
Kenney, J. D. P., Carlstrom, J. E., & Young, J. S. 1993, ApJ, 418, 687
Krugel, E., Steppe, H., & Chini, R. 1990, A&A, 229, 17
Martin, J.-M., Bottinelli, L., Dennefeld, M., & Gouguenheim, L. 1991, A&A, 245, 393
Marx, M., Krugel, E., Klein, U., & Wielebinski, R. 1994, A&A, 281, 718
Mazzarella, J. M., & Balzano, V. A. 1986, ApJS, 62, 751
Mazzarella, J. M., & Boroson, T. A. 1993, ApJS, 85, 27
Mazzarella, J. M., Bothun, G. D., & Boroson, T. A. 1991, AJ, 101, 2034
Regan, M. W., Sheth, K., & Vogel, S. N. 1999, ApJ, 526, 97
Regan, M. W., Thornly, M. D., Helfer, T. T., et al. 2001, ApJ, 561, 218
Sage, L. J. 1993, A&A, 272, 123
Sakamoto, K., Okumura, S. K., Ishizuki, S., & Scoville, N. Z. 1999, ApJS, 124, 403
Sanders, D. B., Scoville, N. Z., & Soifer, B. T. 1988, ApJ, 335, L1
Sanders, D. B., Scoville, N. Z., & Soifer, B. T. 1991, ApJ, 370, 158
Sofue, Y. 1996, ApJ, 458, 120
Sofue, Y. 1997, PASJ, 49, 17
Sofue, Y., & Rubin, V. 2001, ARA&A, 39, 137
Sofue, Y., Tutui, Y., Honma, M., et al. 1999, ApJ, 523,136
Sofue, Y., Wakamatsu, K., Taniguchi, Y., & Nakai, N. 1993, PASJ, 45, 43
Solomon, P. M., Downes, D., & Radford, S. J. E. 1992, ApJ, 387, L55
Stine, P. C. 1992, ApJS, 81, 49
Taniguchi, Y., Kameya, O., Nakai, N., & Kawara, K. 1990, ApJ, 358, 132
Taniguchi, Y., Kameya, O., & Nakai, N. 1991, Dynamics of Galaxies and Their Molecular Distribution, ed. F. Combes, & F. Casoli (Kluwer Academic Publishers), IAU Symp., 146, 328
Tutui, Y., & Sufue, Y. 1999, A&A, 351, 467
Wiklind, T., & Henkel, C. 1989, A&A, 225, 1
Wong, T., & Blitz, L. 2002, ApJ, 569, 157
Young, J. S., & Scoville, N. Z. 1991, ARA&A, 29, 581
Young, J. S., Lori, A., Kenney, J. D. P., Lesser, A., & Rownd, B. 1996, AJ, 112, 1903
Young, J. S., Xie, S., Kenney, J. D. P., & Rice, W. L. 1989, ApJS, 70, 699
Young, J. S., Xie, S., Tacconi, L., et al. 1995, ApJS, 98, 219